Catalyst performance of novel Pt/Mg(Ga)(Al)O catalysts for alkane dehydrogenation

Georges Siddiqi, Pingping Sun, Vladimir Galvita, Alexis T. Bell *

Department of Chemical Engineering, University of California, Berkeley, CA 94720-1462, USA

ARTICLE INFO

ABSTRACT

The dehydrogenation of ethane and propane using a Pt catalyst supported on a novel Mg(Ga)(Al)O mixed oxide support was investigated. Catalyst performance is strongly dependent on Ga content in the support, a peak in activity for both ethane and propane dehydrogenation occurs at Ga/Pt = 1.4–5.4, and selectivity is a monotonic function of Ga/Pt, reaching nearly 100% at Ga/Pt = 5.4. The addition of hydrogen to the feed resulted in a peak in activity with respect to H_2/alkane. The increase in dehydrogenation rate with H_2 addition is attributed to H-atom-assisted dehydrogenation of alkyl species formed upon dissociative adsorption of the reactant alkane. Beyond the peak in activity with H_2 addition, a further increase in H_2 feed concentration contribute to alkene hydrogenation, thereby reducing the net rate of dehydrogenation. Hydrogen addition to the feed, however, had relatively little effect on alkene selectivity, which remained near 100%. The presence of Ga also suppressed coke formation. Interestingly, less coke was formed during propane dehydrogenation than ethane dehydrogenation, and no correlation was found between coke formation and catalyst deactivation. Thus, the extent of deactivation was lower for ethane than propane dehydrogenation, whereas the amount of coke deposited was higher in the former case. Since the amount of carbon deposited as coke is higher than the amount of exposed Pt, it is concluded that most of the coke resides on the support, and that only a small amount resides on the Pt particles. The higher level of deactivation seen during propane versus ethane dehydrogenation is attributed to a higher coverage of Pt by coke precursors derived from propane than ethane.

1. Introduction

Recent studies have shown that calcined hydrotalcites, referred to as Mg(Al)O, are good supports for Pt-based catalysts for the dehydrogenation of light alkanes to alkenes and hydrogen [1–9]. Such materials are hydrothermally stable and are capable of dispersing small Pt particles due to the presence of Al cations at the support surface [10]. The basic character of the support is also desirable, since it minimizes coke formation. Several investigators have shown, though, that in the absence of a promoter, Pt supported on Mg(Al)O and other supports have poor alkene selectivity and accumulate coke rapidly due to readsorption of the alkene on the Pt surface [8,11–18]. High alkene selectivity, minimal coke formation, and better catalyst activity can be achieved by promoting Pt supported on Mg(Al)O or other supports with elements such as Sn, Ga, and Ge [9,14–16,18].

Hydrotalcites were prepared with Ga cations substituting for Al, i.e., Mg(Ga)(Al)O following the procedure described in [19]. When Pt was dispersed on these materials and reduced at 873 K, Ga^{3+} cations present at the surface of the support were reduced to Ga atoms, which then formed PtGa alloys with the dispersed Pt nanoparticles. The presence of such alloys was confirmed by EXAFS, STEM-EDX, and high-resolution TEM. In this study, we report the performance of Pt/Mg(Ga)(Al)O catalysts for the dehydrogenation of ethane and propane, and we compare the activity, selectivity, stability, and coking characteristics of these catalysts to Pt/Mg(Al)O, PtGa/Mg(Al)O and PtSn/Mg(Al)O.

2. Experimental

2.1. Catalyst preparation

Pt/Mg(Ga)(Al)O catalysts were prepared according to the procedure described in Ref. [19]. The performance of these catalysts was compared with PtSn/Mg(Al)O catalysts. The preparation of the PtSn/Mg(Al)O catalyst was identical to that described by Galvita et al. [9]. In short, Pt was introduced into calcined Mg(Al)O by incipient wetness impregnation of a toluene solution of Pt(acetylacetonate)$_2$ (Sigma Aldrich, 99.99%) dissolved in toluene (2.7 mL toluene/g catalyst). Pt(acac)$_2$ was chosen as the catalyst precursor, since it can be dissolved in an organic solvent. This source of Pt is preferred over an aqueous solution of H_2PtCl_6 which is acidic and as a result leaches Mg and Al from the support. After drying and reduction to form metallic Pt, Sn was added using tetra-n-butyl tin (Alfa Aesar, 94%) dissolved in decane (10 mL solvent/g support)

* Corresponding author. Fax: +1 510 642 4778.
E-mail address: bell@cchem.berkeley.edu (A.T. Bell).

under flowing 10% H_2/Ar atmosphere (120 cc/min) [9]. The catalyst was then dried and reduced. PtGa catalysts were synthesized using the same procedure outlined in Part I, but Ga addition was done using Ga(acetylacetonate)$_3$ (Sigma Aldrich, 99.99%) dissolved in toluene (2.7 mL toluene/g catalyst). The catalyst was dried and reduced in flowing H_2 at 873 K.

2.2. Catalyst testing

Reactions were carried out in a quartz reactor with an inner diameter of 7 mm. Prior to testing, the catalyst (0.025 g, 0.25–0.5 mm particle size, diluted with quartz particles of the same particle size in a 1:4 ratio) was heated at 10 K/min to 873 K in 20% H_2 in He and then maintained at this temperature for 1 h. The catalyst bed was heated by a three-zone furnace (Applied Test System, Inc.) controlled by Watlow 988 controllers. The temperature of the catalyst bed was measured by two thermocouples centered axially inside the reactor, one at the top and one at the bottom of the catalyst bed. Brooks Mass Flow Controllers (MFC) were used to deliver a defined flow of each gas. All experiments were performed in the kinetic regime. Internal mass transport limitations were not observed as evidenced by a linear Arrhenius plot and satisfaction of the Weisz–Prater criterion [20].

Coke deposition occurred during the exposure of the catalyst to ethane or propane. The amount of coke deposited was determined by combustion of the deposited material. Prior to combustion, the catalyst (0.025 g) was purged with flowing He (60 cm^3/min) at 873 K for 5 min, and then exposed it to a mixture of 5% O_2 in He flowing at 60 cm^3/min. The CO_2 generated was monitored by on-line mass spectrometry (MS). The amount of deposited coke was calculated from the amount of generated CO_2. Regeneration of the catalysts was done by oxidizing the catalyst in a flow of 10% O_2 in He (100 cm^3/min) for 20 min and then reducing the catalyst in a flow of 20% H_2 in He (100 cm^3/min) for 30 min. Prior to the changing the gas composition, the reactor was flushed with helium.

For time-on-stream measurements of coke deposition, the catalysts were reduced as described previously, then place under reaction conditions for a set amount of time. Following use, the catalyst was purged with flowing He (60 cm^3/min) at 873 K for 5 min, then exposed it to a mixture of 5% O_2 in He flowing at 60 cm^3/min to burn off coke deposits. CO and CO_2 evolutions were monitored by mass spectrometry. After oxidation, the catalyst was re-reduced for 20 min and then used again.

CO chemisorption by the reduced catalyst was measured as follows. The catalyst was first reduced in a mixture of 20% H_2 in He flowing at 60 cm^3/min while it was heated at 10 K/min to 873 K and then maintained at this temperature for 1 h, after which the gas flow was switched to 60 cm^3/min He, and the catalyst was cooled to 293 K. Pulses (5 cm^3) of 1% CO in He were passed over the catalyst bed, and the effluent pulse was analyzed by mass spectrometry. When no more CO uptake was observed, pulsing was stopped and amount of CO adsorbed was calculated. The catalyst was then heated back up to 873 K in 20% H_2 in He, and upon stabilizing at 873 K either ethane or propane was passed over the catalyst for 2 h. After reaction, the catalyst was cooled under flowing He to 293 K, and pulses of 1% CO in He were passed through the catalyst bed to determine the change in CO adsorption capacity.

Reactants and products were analyzed online using a gas chromatograph-mass spectrometer (Varian, Inc., Model 320) equipped with a 14-port sampling valve and three sample loops. One sample loop was injected into an Alumina PLOT column, and eluting products were detected by a flame ionization detector (FID). The contents of the second sample loop were injected into a second Alumina Plot column and were detected and analyzed by mass spectrometry. The contents of the third sample loop were injected into a Hayesep N column (used to adsorb CO_2, H_2O, and heavy hydrocarbons) connected in series with a Mol Sieve 5A packed column. The products eluting from this column were detected by a thermal conductivity detector (TCD).

The ratio of hydrogen to ethane partial pressure in the feed was varied from 0 to 2.5, while maintaining the total flow constant by appropriate addition of He. Experiments conducted with the empty reactor showed that the conversion of ethane and propane was less than 0.05% at 893 K.

The selectivity to ethene was determined from Eq. (1) and the selectivity to propene was determined from Eq. (2):

$$S_{C2H4} \ (\%) = [C_2H_4]/([C_2H_4] + 0.5[CH_4]) \times 100\% \qquad (1)$$

$$S_{C3H6} \ (\%) = [C_3H_6]/([C_3H_6] + (2/3)[C_2H_4] + (1/3)[CH_4] \\ + (2/3)[C_2H_6]) \times 100\% \qquad (2)$$

Deactivation of the catalysts was calculated by comparing the percentage change in alkene concentration at the outlet between 1 and 120 min time on stream:

$$D_{alkene} = ([alkene]_{1\,min} - [alkene]_{120\,min})/[alkene]_{1\,min} \times 100\% \qquad (3)$$

3. Results

3.1. Ethane dehydrogenation

Fig. 1a and b compares the rate of ethene formation and the selectivity to ethene, respectively, for Pt/Mg(Ga)(Al)O and Pt/Mg(Al)O, as a function of time on stream. Pt/Mg(Ga)(Al)O exhibits an activity at time zero that is 40% higher than that of Pt/Mg(Al)O. The initial ethene selectivity for Pt/Mg(Ga)(Al)O, and Pt/Mg(Al)O is 99%, whereas that for Pt/Mg(Al)O is only 39%, with 61% selectivity to methane. After two hours time on stream, all catalysts deactivate by 3–7%. Selectivity to ethene is a monotonic function, reaching ~100% for Pt/Mg(Ga)(Al)O after 2 h on stream, and reaching 60% for Pt/Mg(Al)O.
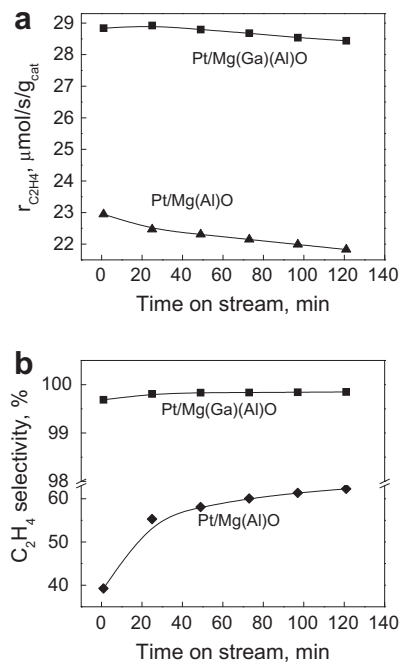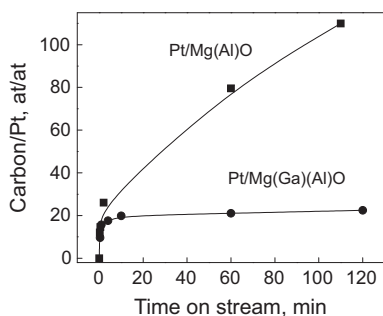

Fig. 1. (a) Comparison of activity of Pt/Mg(Ga)(Al)O (Ga/Pt = 2.86), Pt/Mg(Al)O and (b) selectivity for ethane dehydrogenation. Reaction temperature of 873 K, 20 vol.% C_2H_6 in feed, H_2/C_2H_6 = 1.25, with balance He for total flowrate of 60 ml/min.
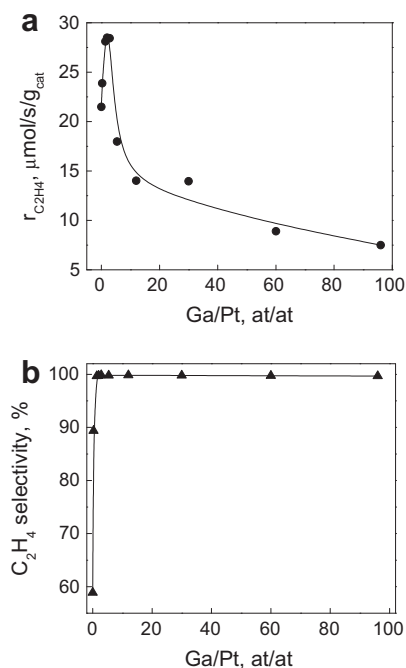
Fig. 2. Carbon formation with time on stream for Pt/Mg(Ga)(Al)O (Ga/Pt = 5.4), Pt/Mg(Al)O for ethane dehydrogenation with reaction temperature of 873 K, 20 vol.% C_2H_6 in feed, H_2/C_2H_6 = 1.25, with balance He for total flowrate of 60 ml/min.

Fig. 4. Carbon formation after 120 min of ethane dehydrogenation at different Ga/Pt ratios, feed composition H_2/C_2H_6 = 1.25. Reaction temperature of 873 K, 20 vol.% C_2H_6 in feed, H_2/C_2H_6 = 1.25, with balance He for total flowrate of 60 ml/min.
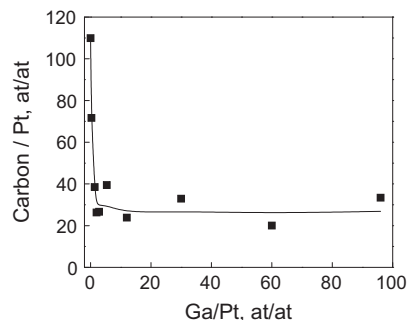
The decrease in activity with time on stream seen in Fig. 1a is accompanied by the buildup of coke, as shown in Fig. 2. After 2 h under reaction conditions, the accumulation of carbon Pt/Mg(Ga)(Al)O reaches a plateau at the equivalent of ~20 C atoms of coke per total Pt atoms, or equivalently ~30 C atoms of coke per exposed Pt atom. By contrast, the formation of coke on Pt/Mg(Al)O increases monotonically, with a final value after 2 h of ~100 C/Pt.

The activity and the selectivity of Pt/Mg(Ga)(Al)O as a function of the bulk Ga/Pt ratio are shown in Fig. 3. With increasing Ga/Pt ratio, the rate of ethene formation increases steadily up to a maximum value for Ga/Pt = 5.4, beyond which the rate of ethene formation decreases monotonically. By contrast, the ethene selectivity increases rapidly with increasing Ga/Pt, reaching a value of nearly 100% for Ga/Pt > 5.4. Fig. 4 shows that the accumulation of coke is also affected by the Ga/Pt ratio; the C/Pt ratio decreases from a value of about 70 in the absence of Ga to a value of about 30 for Ga/Pt > 5.4.

Previous studies have shown that the activity of PtSn/Mg(Al)O can be enhanced by adding H_2 to the feed [8,21,22]. Fig. 5a shows

Fig. 3. The (a) activity and (b) selectivity of different Ga/Pt ratio Pt/Mg(Ga)(Al)O catalysts for ethane dehydrogenation, feed composition H_2/C_2H_6 = 1.25, points recorded after 120 min time on stream. Reaction temperature of 873 K, 20 vol.% C_2H_6 in feed, H_2/C_2H_6 = 1.25, with balance He for total flowrate of 60 ml/min.

that rate of ethene formation over Pt/Mg(Ga)(Al)O increases by approximately tenfold when the ratio of H_2 to C_2H_6 is increased from 0 to 0.26. Above H_2/C_2H_6 = 0.58, the rate of ethene formation decreases monotonically. Fig. 5b shows the effect of H_2/C_2H_6 ratio on the ethene concentration. Also shown in this figure is the equilibrium concentration of ethene. The patterns seen in Fig. 5a and b are very similar to those reported for PtSn/Mg(Al)O [9]. Also similar to what was observed for PtSn/Mg(Al)O, the addition of H_2 to the feed reacted over Pt/Mg(Ga)(Al)O has no effect on the ethene selectivity, which remains at nearly 100%, as seen in Fig. 5c.
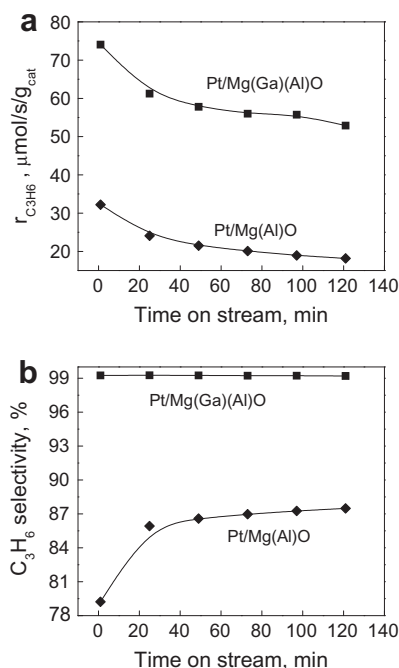
3.2. Propane dehydrogenation

The effects of time on stream on the activity and selectivity of Pt/Mg(Ga)(Al)O and Pt/Mg(Al)O for propane dehydrogenation are presented in Fig. 6. Pt/Mg(Ga)(Al)O exhibit an initial propene activity that is about 2.5 higher than that of Pt/Mg(Al)O. However, after 2 h TOS, Pt/Mg(Ga)(Al)O loses ~30% of its initial activity and Pt/Mg(Al)O looses ~40% of its original activity, a significantly higher extent of deactivation than was observed during ethane dehydrogenation. The propene selectivity was 99% for Pt/Mg(Ga)(Al)O but only 87% for Pt/Mg(Al)O after 2 h of time on stream, with the balance of the products being a mixture of ethane, ethene, and methane. For identical reaction conditions, the rate of propene formation is roughly 2.5 times higher than that for ethene formation for Pt/Mg(Ga)(Al)O, and slightly lower for PtSn/Mg(Al)O, whereas the rate of propene formation to ethene formation was only roughly 1.4 times higher for Pt/Mg(Al)O. A propene selectivity of approximately 99% is achieved on Pt/Mg(Ga)(Al)O, but both the initial and the final selectivities observed for propene were higher than those for ethene produced on Pt/Mg(Al)O.

The decrease in activity with time on stream is again accompanied by a buildup of coke on catalyst, as shown in Fig. 7. Similar to ethane dehydrogenation, Pt/Mg(Al)O formed more coke than Pt/Mg(Ga)(Al)O, and at a slightly faster rate. However, despite the larger deactivation observed during propane dehydrogenation compared to ethane, the total coke buildup after 2 h time on stream was less, for both Pt/Mg(Al)O and Pt/Mg(Ga)(Al)O.
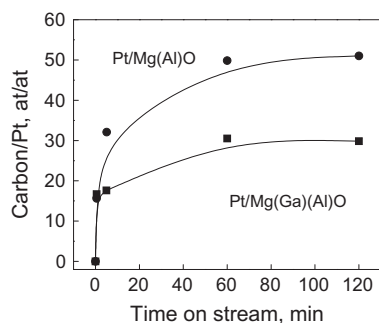
The effect of the Ga/Pt ratio on the activity and selectivity of Pt/Mg(Ga)(Al)O is shown in Fig. 8. As seen in Fig. 3 for ethane dehydrogenation, the activity for propane dehydrogenation reaches a maximum value at Ga/Pt = 5.4; however, the increase in activity relative to Ga/Pt = 0 is nearly 3 for propene dehydrogenation versus only 1.3 for ethane dehydrogenation. The influence of Ga/Pt ratio on propene selectivity also differs from what is seen in Fig. 3b for ethene selectivity. The propene selectivity rises rapidly from 87% to 99% when the Ga/Pt ratio is increased from 0 to 5.4, but then the propene selectivity decreases down to 97% with further increase in Ga/Pt ratio.
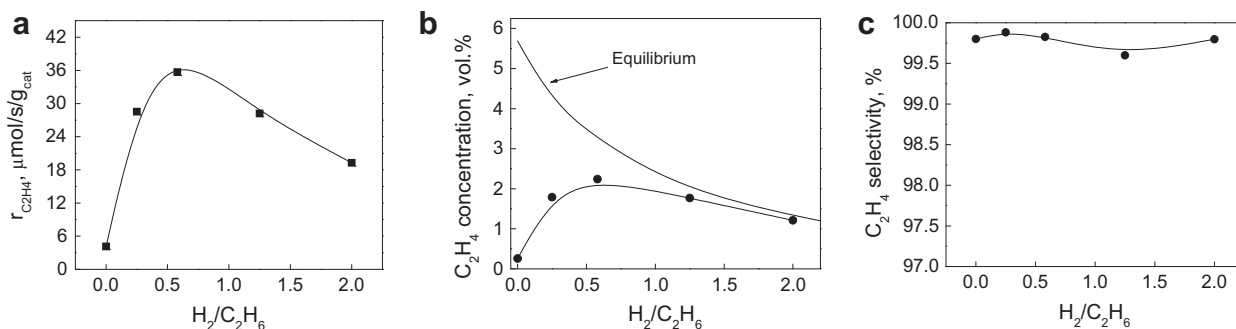
Fig. 5. Effect of feed composition (H_2/C_2H_6) on ethane dehydrogenation. (a) Reactivity, (b) comparison of the vol.% of ethene formed to the equilibrium concentration and (c) selectivity. Total flow kept constant at 60 ml/min by adding a balance of He, T = 873 K.
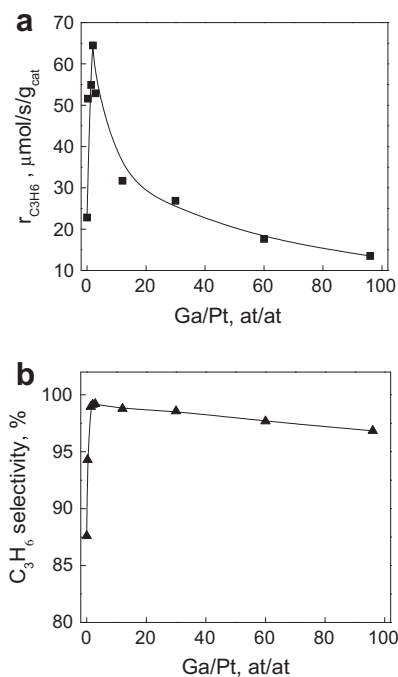

Fig. 6. (a) Comparison of activity of Pt/Mg(Ga)(Al)O (Ga/Pt = 2.86) and Pt/Mg(Al)O and (b) selectivity for propane dehydrogenation. Reaction temperature of 873 K, 20 vol.% C_3H_8 in feed, H_2/C_3H_8 = 1.25, with balance He for total flowrate of 60 ml/min.

Fig. 8. Effect of Ga/Pt ratio on Pt/Mg(Ga)(Al)O catalysts for C_3H_8 dehydrogenation (a) activity and (b) selectivity, feed composition of H_2/C_3H_8 = 1.25 and all data points are after 120 min time on stream. Reaction temperature of 873 K, 20 vol.% C_3H_8 in feed, H_2/C_3H_8 = 1.25, with balance He for total flowrate of 60 ml/min.
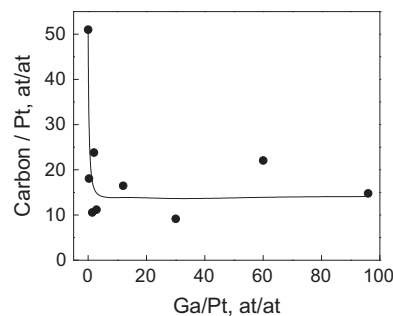

Fig. 7. Carbon formation with time on stream for Pt/Mg(Ga)(Al)O (Ga/Pt = 5.4), Pt/Mg(Al)O for propane dehydrogenation with reaction temperature of 873 K, 20 vol.% C_3H_8 in feed, H_2/C_3H_8 = 1.25, with balance He for total flowrate of 60 ml/min.

Fig. 9. Carbon formation after 120 min of propane dehydrogenation at different Ga/Pt ratios, Reaction temperature of 873 K, 20 vol.% C_3H_8 in feed, H_2/C_3H_8 = 1.25, with balance He for total flowrate of 60 ml/min.

The influence of Ga/Pt ratio on the accumulation of coke for propane dehydrogenation is similar to that observed for ethane dehydrogen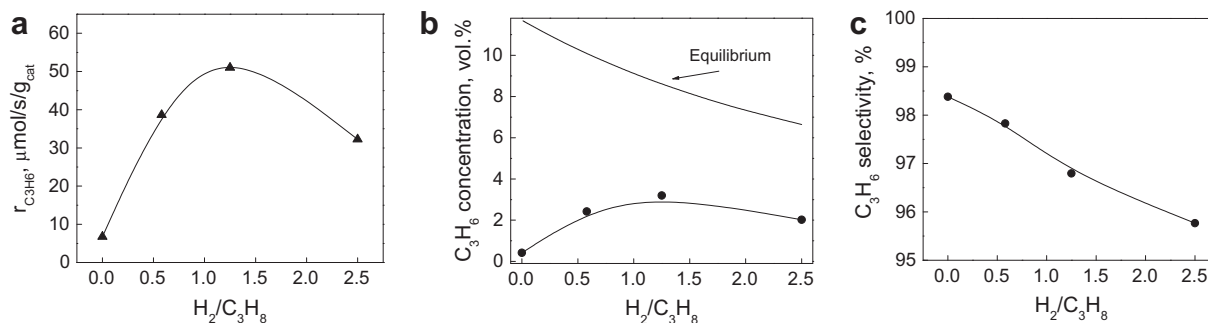ation. Fig. 9 shows that the C/Pt ratio decreases from about 47 to about 15 as the Ga/Pt ratio is increased from 0 to 5.4, and then remains more or less constant for higher Ga/Pt ratios.

Fig. 10. Effect of feed composition (H_2/C_3H_8) on propane dehydrogenation. (a) reactivity, (b) comparison of the vol.% of propene formed to the equilibrium concentration and (c) selectivity. Total flow kept constant at 60 ml/min by adding a balance of He, T = 873 K.

Fig. 11. Effect of reaction cycling on catalyst activity during ethane (below break, Ga/Pt = 5.4) and propane (above break, Ga/Pt = 2.0) dehydrogenation. Each cycle consists of reduction–reaction–oxidation steps. Reaction temperature of 873 K, 20 vol.% alkane in feed, H_2/alkane = 1.25, with balance He for total flowrate of 60 ml/min.
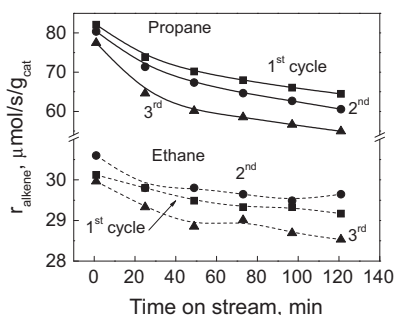
Fig. 10a illustrates the effects of H_2/C_3H_8 ratio on the rate of propene formation and the propene selectivity. The addition of H_2 to the feed causes the rate of propene formation to increase up to a H_2/C_3H_8 ratio of 1.25. It is notable that while the effect of H_2 addition on the rate of propene formation is qualitatively similar to that seen for ethene formation (Fig. 5a), the maximum in propene formation occurs at H_2/C_3H_8 = 1.25, whereas the maximum in ethene formation occurs at H_2/C_2H_6 = 0.58. A plot of the concentration of propene versus at H_2/C_2H_6 ratio is presented in Fig. 10b. Unlike the case of ethene dehydrogenation, the product concentration of propene does not approach that predicted for equilibrium conversion of the feed. The H_2/C_3H_8 ratio has a somewhat larger effect on the selectivity to propene than on the selectivity to ethene produced by ethane dehydrogenation (compare Figs. 10c and 5c), but the propene selectivity still remains above 95.5% even at the highest at H_2/C_3H_8 ratio.

Fig. 11 shows the effects of reduction–reaction–oxidation cycles on catalyst activity during ethane and propane dehydrogenation. For ethane dehydrogenation, there is a slight increase in activity compared to the first cycle after the second, but a decrease in activity in the following third cycle. The loss in activity between the first

and third cycles at 120 min TOS is 2.1%. For propane dehydrogenation, the trend changes to a constant decrease in activity with repeated cycles, the loss in activity between the first and third cycles after 120 min TOS amounting to 14.8%.

The activity, selectivity, deactivation, and carbon formation after 2 h TOS is presented in Table 1 for Pt, PtSn, and PtGa supported on Mg(Al)O) and for Pt/Mg(Ga)(Al)O. For ethane dehydrogenation, Pt/Mg(Ga)(Al)O, PtSn/Mg(Al)O, and PtGa/Mg(Al)O display comparable activity, selectivity, and deactivation; however, the deposition of coke is 50% less than that observed for the other three catalysts. Pt/Mg(Ga)(Al)O creates about 50% less coke. Pt/Mg(Ga)(Al)O also exhibits superior activity for propane dehydrogenation, as well as less coke buildup and a lower extent of deactivation. In all cases, modified catalysts have higher activity, and selectivity, and lower deactivation and coke formation than Pt/Mg(Al)O.

4. Discussion

4.1. Catalyst activity and selectivity

Figs. 3 and 8 show a strong dependence of the rates of ethene and propene formation as a function of the bulk Ga/Pt ratio in Pt/Mg(Ga)(Al)O. The maximum activity in both cases is reached for Ga/Pt = 2.0, but the maximum activity is more than twofold higher for propane dehydrogenation than ethane dehydrogenation, under equivalent reaction conditions. The alkene selectivity for both systems reaches nearly 100% at Ga/Pt = 5.4. However, while the selectivity to ethene remains constant for higher Ga/Pt ratios, the selectivity to propene decreases slowly. In Part I of this work it was shown that upon H_2 reduction of Pt/Mg(Ga)(Al)O at 873 K, Ga^{3+} cations present near the surface of the support are reduced and form PtGa alloys, the amount of Ga associated with the Pt increasing with increasing bulk Ga/Pt ratio [19]. Therefore, the effects observed in Figs. 3 and 8 can be attributed to the formation of PtGa alloys. What is not known, however, is the Ga/Pt ratio at the surface of the bimetallic particles and, hence, it is not possible to relate the effects of surface Ga/Pt ratio to catalyst activity and selectivity.

Table 1
Comparison activity, selectivity toward the alkene product, deactivation and coke formation of Pt, PtSn, and PtGa catalyst supported on Mg(Al)O to Pt/Mg(Ga)(Al)O.

Catalyst	M/Pt	Activity, μmol/s/g_cat		Selectivity, %		Deactivation, %		C/Pt, at/at	
		C_2	C_3	C_2	C_3	C_2	C_3	C_2	C_3
Pt/Mg(Al)O	0	21.8	18.2	62.3	87.5	4.8	43.6	110	51
Pt/Mg(Ga)(Al)O	2.86	28.4	52.9	99.9	99.2	1.4	28.6	27	11
PtSn/Mg(Al)O	0.6	27.0	46.6	98.5	98.7	2.4	38.8	54	38
PtGa/Mg(Al)O	3	18.5	25.6	97.2	98.2	21.5	54.7	48	25

The observation of a maximum in catalyst activity with increasing Ga/Pt ratio very likely reflects the influence of a monotonic decrease in the size of Pt ensembles present at the surface of the supported metal particles, together with electronic effects caused by the presence of Ga atoms at the catalyst surface. A similar phenomenon has been observed for ethane dehydrogenation on PtSn/Mg(Al)O, albeit the peak in activity is not as sharp as that seen for Ga in Fig. 3 [9]. Studies of PtSn alloys have also shown that the presence of Sn reduces the energy of adsorption for ethene, thereby minimizing the readsorption of ethene and the subsequent dissociation of the C–C bond to form CH_x species [23–25]. These CH_x species contribute to the formation of CH_4 and to the loss in ethene selectivity. As was shown previously for PtSn/Mg(Al)O, CH_x species formed from the readsorption of ethene are responsible for the deposition of coke [8,9]. It is quite plausible then to propose that the addition of Ga to Pt has similar effects to those of Sn.

The notably higher activity of Pt/Mg(Ga)(Al)O (Ga/Pt = 2.86) for propane versus ethane dehydrogenation is likely due to the easier initiation of the later reaction. As discussed in Ref. [9], the rate-limiting step for alkane dehydrogenation is dissociative adsorption of the alkane to form adsorbed alkyl species and atomic hydrogen. Since the C–H bond of the methylene group in propane is weaker than the C–H bond of the methyl group in ethane, initiation of propane should occur more easily than for ethane, resulting in a higher rate of propane dehydrogenation.

The ratio of H_2 to alkane influences the activity and selectivity of alkene formation on Pt/Mg(Ga)(Al)O (Ga/Pt = 5.4) (see Figs. 5 and 10). This effect was noted earlier in our studies of ethane and propane dehydrogenation on Pt/Mg(Al)O and PtSn/Mg(Al)O [9]. In all cases, the rate of alkene formation increases with increasing H_2/alkane ratio and then passes through a maximum. In our studies of ethane dehydrogenation on Pt/Mg(Al)O and PtSn/Mg(Al)O, we proposed that at low hydrogen partial pressures the increase in adsorbed H atoms on the catalyst surface contributes to the removal of the second hydrogen atom from adsorbed alkyl species, thereby accelerating the rate of alkene formation [9]. At much higher hydrogen partial pressures, hydrogenation of the nascent alkyl species becomes more significant, leading to reformation of the alkane and a decrease in the rate of alkene formation. As this latter process occurs, the overall concentration of alkene in the products approaches that expected at equilibrium.

4.2. Carbon formation and deactivation

A loss in alkane dehydrogenation activity and the accumulation of coke was observed with time on stream for all the catalysts investigated in this study. Similar patterns were noted in our study on ethane dehydrogenation of Pt/Mg(Al)O and PtSn/Mg(Al)O [9]. In the present work, it was found that the loss in activity for ethane dehydrogenation after 2 h on stream was minimal (~3%) in the case of Pt, PtSn, and PtGa supported on Mg(Al)O and Pt/Mg(Ga)(Al)O but much more significant in the case of propane dehydrogenation (~25–45%) (Table 1). The presence of Ga compared to Sn reduced the deactivation and the amount of coke deposited during both ethane and propane dehydrogenation. The results presented in Figs. 1, 4, 6 and 9 demonstrate that there is no correlation between loss in dehydrogenation activity and coke accumulation. Moreover, the ratios of deposited carbon to surface Pt atoms are much greater than unity in all cases. This suggests that the most of the accumulated coke is present on the support and that only a small fraction remains on the surface of the metal particles. The loss of dehydrogenation activity due to sintering of the metal particles is likely minimal. This conclusion is based on the observation that the loss in activity after three cycles for ethane dehydrogenation is only 2.1% (and an increase in activity was noted during

the second cycle). While the final loss in activity for propane dehydrogenation after three cycles was 14.8%, the loss in initial activity after each cycle was minimal (Fig. 11). These results lead suggest that catalyst deactivation may be due to the accumulation of a small amount of coke on the active metal particles, while most of the coke lies on the support.

Further insights into the differences in carbon formation between ethane and propane dehydrogenation with Pt can be drawn from surface sciences investigations of ethene and propene. Studies on Pt(1 1 1) and Sn/Pt(1 1 1) surfaces have shown that the energies of adsorption for ethene and propene on Pt(1 1 1) differ negligibly [23,24,26]. In an inert atmosphere, the extent of propene decomposition on Sn/Pt(1 1 1) surfaces is higher than that of ethene for all Sn coverages tested (0–0.33) [24]. However, as noted previously, when H_2 is adsorbed onto the surface of Pt(1 1 1), the decomposition product of propene, propylidyne, is rehydrogenated far more readily than ethylidyne [27,28]. Thus, the adsorption of H_2 is not only crucial to reducing the amount of coke formed on the catalysts, via the hydrogenation of coke precursor species, but also accounts for the lower coke formation noted during propane dehydrogenation compared to ethane dehydrogenation. The effects of Sn in Sn/Pt(1 1 1) on the adsorption energies of ethene and propene show that the main electronic effect of the modifier is to reduce the desorption barriers of the desired products, and given the qualitative agreement in catalyst activity between PtSn/Mg(Al)O and Pt/Mg(Ga)(Al)O, we hypothesize that the manner in which Ga affects the surface is similar to that of Sn (Table 1) [24].

It has been shown that the overall amount of coke formed is greater during ethane dehydrogenation than during propane, but the deactivation is greater during propane dehydrogenation than during ethane; therefore, the total amount of coke formed cannot be responsible for the increased deactivation. However, it is possible that the transfer of carbonaceous species from the metal active site to the support may be less efficient for such species originating from propane than those originating from ethane. The amount of CO chemisorbed before and after alkane dehydrogenation for 2 h was measured for Pt/Mg(Ga)(Al)O (Ga/Pt = 5.4) in an attempt to determine the loss in active sites. The data in Table 2 show after ethane 44% sites capable of CO chemisorption are lost after ethane dehydrogenation, but 98% of such sites are lost after propane dehydrogenation. While these data show a qualitative correlation between loss of CO chemisorption sites and dehydrogenation activity, the loss in CO chemisorptions capacity is greater than the loss in dehydrogenation activity for both alkanes. We hypothesize that coke not only alters the number of sites for CO adsorption, but also decreases the heat of CO adsorption. Consistent with the latter idea, CO adsorption experiments on Pt(1 1 1), (5 5 7) and (13, 1, 1) surfaces before and after hydrocarbon reactions have shown that there is a decrease in the CO desorption temperature after hydrocarbon reaction, indicating that the deposited carbonaceous species weaken the binding of CO [29,30]. Thus, we conclude that the more significant decrease in CO chemisorption than decrease in activity is due to carbon on the surface decreasing the binding energy of CO, and not entirely because of surface coverage by carbon. Our measurements of the loss in CO chemisorptions capacity do show, however, that more

Table 2
Percentage change in amount of CO adsorbed by Pt/Mg(Ga)(Al)O (Ga/Pt = 5.4) before and after TOS = 2 h of either ethane or propane dehydrogenation.

	Change in exposed surface sites, %
Ethane Dehydrogenation	44
Propane Dehydrogenation	98

of the metal surface is affected by carbonaceous species derived from propane that from ethane. Thus, we hypothesize that less mobile coke species derived from propane are responsible for a larger coke buildup on the active metal particles, and hence a larger deactivation.

5. Conclusion

We have shown that Pt/Mg(Ga)(Al)O catalysts prepared by the method described in Part I of this work leads to an active alkane dehydrogenation catalyst that is highly selective for the formation of ethene and propene from ethane and propane, respectively. We have also shown that Pt/Mg(Ga)(Al)O catalysts exhibit lower deactivation and coke formation than conventional bimetallic catalysts, such as PtSn/Mg(Al)O and PtGa/Mg(Al)O. The enhanced activity, selectivity, and resistance to coke formation of the Ga-modified Pt catalysts are attributed to the formation of PtGa alloys. In Part I of this series it was shown that such alloys are formed upon reduction of Pt/Mg(Ga)(Al)O at 873 K. The peak in activity seen for bulk Ga/Pt ratios of 1.4–5.4 is attributed to dilution of Pt ensembles by Ga, which enhance the adsorption of the reactant alkane and inhibits the adsorption of product alkene. Suppressing the latter process is important, since it contributes to the formation product hydrogenolysis (e.g. the conversion of ethene to methane). Adding H_2 to the feed increases the rate of alkene formation due to enhanced hydrogen-assisted dehydrogenation of surface alkyl species. However, as the concentration of alkene in the product approaches the equilibrium concentration, the rate of alkene formation approaches that expected for equilibrium conversion of the alkane and the rate of alkene formation decreases with increasing H_2/alkane ratio. The loss in activity of Pt/Mg(Ga)(Al)O with time on stream is smaller for ethane than propane dehydrogenation. Coke accumulation with time on stream is greater for ethane than propane dehydrogenation, and the moles of carbon deposited on the catalyst are many times higher than the moles of exposed Pt atoms. The lack of correlation between extent of deactivation and carbon formation suggests that only a small fraction of the accumulated coke resides on the surface of the Pt particles and that the bulk accumulates on the support. The lower coke formation during propane dehydrogenation compared to ethane dehydrogenation is attributed to the greater ease of hydrogenation of propylidyne compared to ethylidyne, whereas the disparity between decreased coke formation and increased deactivation observed during propane dehydrogenation is attributed to a greater coverage of the surface of the active metal particle by coke.

References

[1] R.J. Rennard, J. Freel, Journal of Catalysis 98 (1986) 235–244.
[2] Y. Wang, B. Shi, R.D. Guthrie, B.H. Davis, Journal of Catalysis 170 (1997) 89–95.
[3] H. Armendáriz, A. Guzmán, J.A. Toledo, M.E. Llanos, A. Vázquez, G. Aguilar-Rìos, Applied Catalysis A: General 211 (2001) 69–80.
[4] L. Bednarova, C.E. Lyman, E. Rytter, A. Holmen, Journal of Catalysis 211 (2002) 335–346.
[5] S.A. Bocanegra, A. Guerrero-Ruiz, S.R. de Miguel, O.A. Scelza, Applied Catalysis A: General 277 (2004) 11–22.
[6] A. Virnovskaia, S. Jørgensen, J. Hafizovic, Ø. Prytz, E. Kleimenov, M. Hävecker, H. Bluhm, A. Knop-Gericke, R. Schlögl, U. Olsbye, Surface Science 601 (2007) 30–43.
[7] A. Virnovskaia, S. Morandi, E. Rytter, G. Ghiotti, U. Olsbye, The Journal of Physical Chemistry C 111 (2007) 14732–14742.
[8] A. Virnovskaia, E. Rytter, U. Olsbye, Industrial and Engineering Chemistry Research 47 (2008) 7167–7177.
[9] V. Galvita, G. Siddiqi, P. Sun, A.T. Bell, Journal of Catalysis 271 (2010) 209–219.
[10] J.I. Di Cosimo, V.K. Díez, M. Xu, E. Iglesia, C.R. Apesteguía, Journal of Catalysis 178 (1998) 499–510.
[11] D. Sanfilippo, I. Miracca, Catalysis Today 111 (2006) 133–139.
[12] R. Burch, L.C. Garla, Journal of Catalysis 71 (1981) 360–372.
[13] N. Iwasa, T. Akazawa, S. Ohyama, K. Fujikawa, N. Takezawa, Reaction Kinetics and Catalysis Letters 55 (1995) 245–250.
[14] E.L. Jablonski, A.A. Castro, O.A. Scelza, S.R. de Miguel, Applied Catalysis A: General 183 (1999) 189–198.
[15] B. Coq, A. Tijani, F. Figuéras, Journal of Molecular Catalysis 71 (1992) 317–333.
[16] S.A. Bocanegra, A.A. Castro, O.A. Scelza, S.R. de Miguel, Applied Catalysis A: General 333 (2007) 49–56.
[17] S.M. Stagg, C.A. Querini, W.E. Alvarez, D.E. Resasco, Journal of Catalysis 168 (1997) 75–94.
[18] O.A. Bariås, A. Holmen, E.A. Blekkan, Journal of Catalysis 158 (1996) 1–12.
[19] P. Sun, G. Siddiqi, V. Galvita, M. Chi, A.T. Bell, Journal of Catalysis, in press, doi:10.1016/j.jcat.2010.06.017.
[20] P.B. Weisz, C.D. Prater, V.I.K. W.G. Frankenburg, E.K. Rideal, Advances in Catalysis, Academic Press, pp. 143–196.
[21] C. Yu, Q. Ge, H. Xu, W. Li, Industrial and Engineering Chemistry Research 46 (2007) 8722–8728.
[22] M. Tasbihi, F. Feyzi, M.A. Amlashi, A.Z. Abdullah, A.R. Mohamed, Fuel Processing Technology 88 (2007) 883–889.
[23] M.T. Paffett, S.C. Gebhard, R.G. Windham, B.E. Koel, Surface Science 223 (1989) 449–464.
[24] Y.-L. Tsai, C. Xu, B.E. Koel, Surface Science 385 (1997) 37–59.
[25] J.F. Weaver, A.F. Carlsson, R.J. Madix, Surface Science Reports 50 (2003) 107–199.
[26] D.F. Ogletree, H. Bluhm, G. Lebedev, C.S. Fadley, Z. Hussain, M. Salmeron, Review of Scientific Instruments 73 (2002) 3872–3877.
[27] P.S. Cremer, X. Su, Y.R. Shen, G.A. Somorjai, The Journal of Physical Chemistry 100 (1996) 16302–16309.
[28] P.S. Cremer, X. Su, Y.R. Shen, G.A. Somorjai, Journal of the American Chemical Society 118 (1996) 2942–2949.
[29] S.M. Davis, F. Zaera, G.A. Somorjai, Journal of Catalysis 77 (1982) 439–459.
[30] M. Abon, J. Billy, J.C. Bertolini, B. Tardy, Surface Science 167 (1986) 1–17.